Weber looks at the potential for PET in improving the efficiency of the drug development process, focusing on heat shock protein 90, a molecular chaperon involved in protein folding in cellular signaling, proliferation, invasion, and angiogenesis. . . . . ***Page 735***

O'Donnell highlights the possibilities of cancer cell–targeting radiopharmaceuticals and previews an article in this issue on a novel radiolabeled monoclonal antibody approach with nuclear localizing sequences. . . . . ***Page 738***

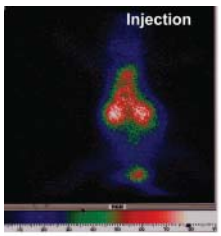

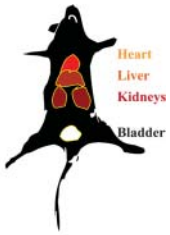

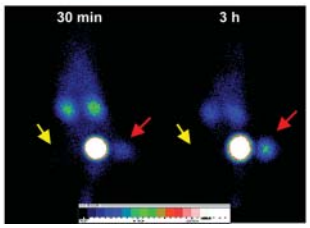

Van Laere and colleagues apply ^{18}F-FDG PET to an exploration of the mechanisms behind beneficial effects observed in patients undergoing high-frequency anterior capsular stimulation for treatment of refractory obsessive–compulsive disorder. . . . . ***Page 740***

Newberg and colleagues measure the whole-body biokinetics and radiation dosimetry of ^{123}I-IMPY and report on the pharmacologic safety of this novel radiopharmaceutical that selectively binds to amyloid plaques in Alzheimer's disease. . . . . ***Page 748***

Schöder and colleagues report on the utility and limitations of ^{18}F-FDG PET/CT in identifying lymph node metastases in a segment of patients with oral cancer and clinically and radiographically negative neck findings. . . . . ***Page 755***

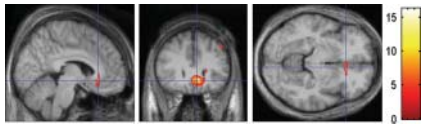

Beer and colleagues describe dosimetry studies with ^{18}F-galacto-RGD, a novel PET tracer for imaging of $\alpha v\beta 3$ expression, in a group of patients with various cancers. . . . . ***Page 763***

de Geus-Oei and colleagues explore the potential of ^{18}F-FDG PET for reducing the number of unnecessary hemithyroidectomies in the preoperative assessment of thyroid nodules in patients with inconclusive fine-needle aspiration biopsy results. . . . . ***Page 770***

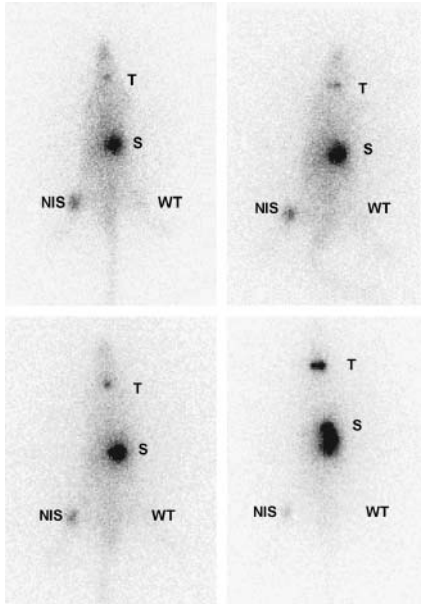

Floeth and colleagues assess the differential diagnostic value of PET using ^{18}F-FET in patients with newly diagnosed solitary intracerebral lesions showing ring enhancement on contrast-enhanced MRI. . . . . ***Page 776***

Millet and colleagues describe a novel quantitative approach with SPECT to study the interaction between ^{123}I-IMZ and benzodiazepine receptors. . . . . ***Page 783***

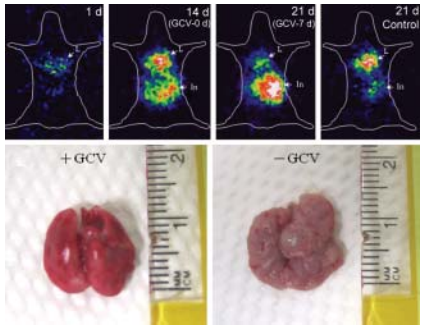

Smith-Jones and colleagues compare ^{68}Ga-DOTA-F(ab′)$_2$-herceptin PET and ^{18}F-FDG PET in a mouse model in predicting tumor response to 17AAG, one of a new class of drugs currently in early clinical trials for breast cancer. . . . . ***Page 793***

Hoffmann and colleagues provide detailed information on performing state-of-the-art coronary CT angiography, including patient preparation, image acquisition, and evaluation techniques, and review potential clinical applications and limitations. . . . . ***Page 797***

Uusijärvi and colleagues investigate the suitability of several electron- and positron-emitting radiolanthanides for radionuclide therapy, with special reference to dosimetric and production possibilities. . . . . ***Page 807***

Frankle and colleagues define an optimal analytic method to derive accurate

serotonin transporter receptor parameters with ^{11}C-DASB PET, a technique with promise in enhancing the quality of information derived in clinical studies of depression, schizophrenia, and addictive behaviors. . . . . ***Page 815***

Chen and colleagues report on toxicity studies of the anti-CD33 monoclonal antibody, HuM195, modified with targeting peptides and labeled with ^{111}In and discuss the promise of this agent in targeted radiotherapy for acute myeloid leukemia. . . . . ***Page 827***

Cho and colleagues describe in vitro evaluations using ^{3}H-AMP with tumor cell lines to explore the potential of ^{11}C-AMP for targeting the nucleoside transport pathway in PET imaging of tumors. . . . .***Page 837***

Tolmachev and colleagues perform in vitro and in vivo studies to determine whether an ^{111}In-labeled affibody molecule

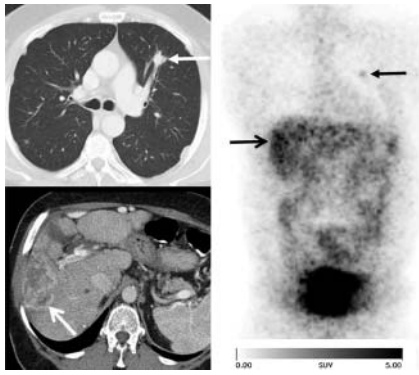

can be used for imaging HER2 overexpression and discuss the implications for imaging and targeted therapy of breast cancer. . . . . ***Page 846***

Chen and colleagues explore the feasibility of radioiodine therapy involving the targeting of hepatoma cells by tissue-specific expression of the human sodium/iodide symporter gene directed by the murine albumin enhancer and promoter. . . . . ***Page 854***

Hosokawa and colleagues report on a method for identifying coronary vulnerable plaques with a catheter-based intravascular radiation detector and ^{18}F-FDG. . . . . ***Page 863***

Khaw and colleagues investigate the use of bispecific antibody complexes and ^{99m}Tc-labeled negatively charged polymers for in vivo visualization of very small atherosclerotic lesions in a mouse model. . . . . ***Page 868***

Deng and colleagues describe the use of ^{131}I-FIAU for assessing lung metastases in a mouse model and discuss the implications for future nuclear medicine techniques to monitor the efficacy of gene delivery and expression. . . . . ***Page 877***

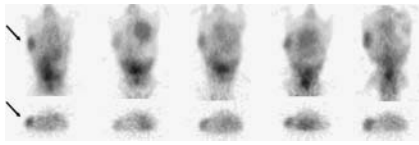

Delbeke and colleagues present the full text of a new SNM guideline compiled to assist physicians in recommending, performing, interpreting, and reporting the results of ^{18}F-FDG PET/CT for oncologic imaging of adult and pediatric patients. . . . . ***Page 885***

ON THE COVER

Images illustrating ^{18}F-FET PET findings false positive for malignancy in a 50-y-old woman with a demyelinating lesion. MRI (top left) shows a ring-enhancing lesion; ^{18}F-FET PET (top right) shows significant uptake, indicating neoplasia; photomicrography of a CD68-immunostained biopsy specimen (bottom left) shows an acute demyelinating lesion with massive invasion of macrophages; and immunohistochemistry for neurofilaments (bottom right) shows persisting axonal processes but also axonal damage within the lesion.

SEE PAGE 780